

ATP-Gated Ionotropic P2X7 Receptor Controls Follicular T Helper Cell Numbers in Peyer's Patches to Promote Host-Microbiota Mutualism

Michele Proietti,^{1,11} Vanessa Cornacchione,^{1,2,11} Tanja Rezzonico Jost,¹ Andrea Romagnani,^{1,3} Caterina Elisa Faliti,^{1,3} Lisa Perruzza,^{1,3} Rosita Rigoni,¹ Enrico Radaelli,⁴ Flavio Caprioli,^{5,6} Silvia Preziuso,⁷ Barbara Brannetti,² Marcus Thelen,¹ Kathy D. McCoy,⁸ Emma Slack,⁹ Elisabetta Traggiai,² and Fabio Grassi^{1,10,*}

¹Institute for Research in Biomedicine, Via Vincenzo Vela 6, 6500 Bellinzona, Switzerland

²Novartis Institute for Biomedical Research, Fabrickstrasse 2, 4002 Basel, Switzerland

³Graduate School for Cellular and Biomedical Sciences, University of Bern, Freiestrasse 1, 3012 Bern, Switzerland

⁴Fondazione Filarete, Viale Ortles 22/4, 20139 Milan, Italy

⁵Department of Pathophysiology and Transplantation, University of Milan, Via Francesco Sforza 35, 20122 Milan, Italy

⁶Unit of Gastroenterology 2, Fondazione IRCCS Ca' Granda, Ospedale Policlinico di Milano, Via Francesco Sforza 35, 20122 Milan, Italy

⁷Department of Veterinary Medical Sciences, University of Camerino, Via Circonvallazione 93/95, 62024 Matelica, Italy

⁸Maurice Müller Laboratories, Universitätsklinik für Viszerale Chirurgie und Medizin (UVCM), University of Bern, Murtenstrasse 35, 3010 Bern, Switzerland

⁹Institute of Microbiology, ETH Zurich, HCI F 413 Vladimir-Prelog-Weg 1-5/10, 8093 Zurich, Switzerland

¹⁰Department of Medical Biotechnology and Translational Medicine, University of Milan, Via G.B. Viotti 3/5, 20133 Milan, Italy

¹¹Co-first author

*Correspondence: fabio.grassi@irb.usi.ch

<http://dx.doi.org/10.1016/j.immuni.2014.10.010>

SUMMARY

Microbial colonization of the gut induces the development of gut-associated lymphoid tissue (GALT). The molecular mechanisms that regulate GALT function and result in gut-commensal homeostasis are poorly defined. T follicular helper (Tfh) cells in Peyer's patches (PPs) promote high-affinity IgA responses. Here we found that the ATP-gated ionotropic P2X7 receptor controls Tfh cell numbers in PPs. Lack of P2X7 in Tfh cells enhanced germinal center reactions and high-affinity IgA secretion and binding to commensals. The ensuing depletion of mucosal bacteria resulted in reduced systemic translocation of microbial components, lowering B1 cell stimulation and serum IgM concentrations. Mice lacking P2X7 had increased susceptibility to polymicrobial sepsis, which was rescued by Tfh cell depletion or administration of purified IgM. Thus, regulation of Tfh cells by P2X7 activity is important for mucosal colonization, which in turn results in IgM serum concentrations necessary to protect the host from bacteremia.

INTRODUCTION

Host physiology and diet influence the development of the gut ecosystem (Muegge et al., 2011). Reciprocally, through interactions with the host, the gut microbiota influences physiology and disease susceptibility (Lozupone et al., 2012), a beneficial homeostatic relationship that is ensured by several layers of control, including mucus, antimicrobial factors, and innate and adaptive immunity (Henao-Mejia et al., 2012; Littman and Pamer, 2011; Sun et al., 2007; Vaishnava et al., 2011).

The gut microbiota promote the development of the gut-associated lymphoid tissue (GALT) (Macpherson and Harris, 2004), which is responsible for intestinal IgA production in response to microbial stimulation (Cerutti and Rescigno, 2008; Craig and Cebra, 1971). In the Peyer's patches (PPs) of the small intestine, T follicular helper (Tfh) cells support affinity maturation of B cells in germinal centers (GCs) (Crotty, 2011) and differentiation of B cells to IgA-secreting plasma cells, a process that is critical in maintaining intestinal homeostasis and efficient mucosal defense (Wei et al., 2011). Moreover, some evidence suggests that affinity maturation of IgA can also affect systemic immunity. For example, it has been shown that recognition of luminal bacteria by secretory IgA prevents their access to the lamina propria and systemic proinflammatory stimulation by bacterial products (Johansen et al., 1999; Macpherson and Uhr, 2004; Sait et al., 2007), a result in agreement with the observation that IgA with reduced bacterial binding capacity results in systemic hyperactivation of the immune system (Kawamoto et al., 2012).

Purinergic receptors in the plasma membranes of eukaryotic cells comprise ATP-gated ionotropic P2Xs (P2X1-7) and guanine nucleotide-binding protein (G protein)-coupled P2Ys (P2Y1, 2, 4, 6, 11-14, which bind also ADP, UDP, UTP, or UDP-glucose) (Burnstock, 2007). ATP released during tissue damage acts as a danger-associated molecular pattern (DAMP) for cells of the innate immune system through stimulation of P2 receptors. P2rx7, which encodes the ATP-gated P2X7 receptor, is a signature gene of effector T cell subsets (Choi et al., 2013; Gavin et al., 2007; Hale et al., 2013; Hill et al., 2008). We have previously shown that P2X7 activity regulates the immunosuppressive function of regulatory T (Treg) cells (Schenk et al., 2011), and persistent P2X7 stimulation by ATP results in pyroptosis-like cell death of Treg cells (Taylor et al., 2008). In fact, sustained P2X7 activation leads to the formation of a pore permeable to molecules up to 900 Da.

We found that *P2rx7* is selectively and highly expressed in Tfh cells. Deletion of *P2rx7* in Tfh cells resulted in resistance to cell death, enhanced GC reaction in PPs, increased IgA binding to commensals, and reduction of mucosal bacteria. Our results unravel P2X7 as a regulator of the adaptive IgA response in the small intestine to allow commensalism and systemic stimulation of the immune system.

RESULTS

Tfh Cell Numbers Are Increased in the PPs of *P2rx7*^{-/-} Mice

Histochemical analysis of the intestine from *P2rx7*^{-/-} mice revealed enlarged PPs with increased cellularity as compared to wild-type (WT) mice (Figure 1A); ileal and colonic epithelium were otherwise histologically normal (Figure S1A available online). Flow cytometry of cells from *P2rx7*^{-/-} PPs revealed an increase of Tfh cells identified by expression of the C-X-C chemokine receptor type 5 (CXCR5) (Förster et al., 1996), CD28 family member inducible T cell costimulator (ICOS) (Choi et al., 2011), the transcription factor B cell lymphoma 6 (Bcl6) (Nurieva et al., 2009; Yu et al., 2009), programmed cell death-1 (PD1) (Haynes et al., 2007), and CD40L (Figure 1B). In addition to the increase in Tfh cell numbers, mean fluorescence intensities (MFIs) of ICOS and CD40L were increased in Tfh cells from *P2rx7*^{-/-} mice (Figure 1C). Quantitative real-time PCR on various cell subsets purified from PPs of WT mice, namely CD19⁺ B cells, Fas⁺PNA⁺ GC B cells, CD3⁺CD4⁺ T cells, Treg cells, and Tfh cells, revealed highest expression of *P2rx7* transcripts in Tfh cells (Figure 1D). P2X7 was the only P2X receptor subtype expressed in PPs Tfh cells (Figure 1E). In fact, these cells showed the strongest response to stimulation with the P2X7 agonist 3'-O-(4-Benzoyl)benzoyl ATP (BzATP) (see below). In Tfh cells isolated from *P2rx7*^{-/-} PPs, we observed higher expression of *Bcl6* transcripts and concomitant reduction in transcripts encoding the *Bcl6* antagonist *Blimp1* (Figure 1F; Johnston et al., 2009). Expression of *Bcl6* inhibits CD4 T cell polarization toward T helper 1 (Th1) and Th17 phenotypes (Nurieva et al., 2009; Yu et al., 2009). Accordingly, the Th17-cell-specific transcripts *Rorc* and *Il17a* and Th1-cell-specific transcripts *Tbx21* and *Ifng* were all reduced in Tfh cells from *P2rx7*^{-/-} PPs (Figure 1F).

The activity of the P2X7 receptor is influenced by a strain polymorphism (P451L) in the cytoplasmic domain. Proline-bearing BALB/c mice are more sensitive to P2X7 stimulation by ATP than leucine-bearing C57BL/6 mice (Adriouch et al., 2002). We observed a progressive increase in Tfh cells across BALB/c, C57BL/6, and finally *P2rx7*^{-/-} mice, indicating that P2X7 responsiveness inversely correlates with Tfh cell number (Figure S1B). These observations suggest that P2X7 activity limits the abundance of Tfh cells in PPs.

Expansion of Tfh Cells in PPs of *P2rx7*^{-/-} Mice Is Cell Intrinsic

To rule out that other cell subsets contributed to the increase of Tfh cell numbers in PPs from *P2rx7*^{-/-} mice, we adoptively transferred either WT or *P2rx7*^{-/-} CD4 Foxp3^{EGFP} T cells into *Cd3e*^{-/-} mice. This model of transfer into lymphopenic mice has previously demonstrated selective conversion of FoxP3-expressing cells into Tfh cells in PPs (Tsuji et al., 2009).

Foxp3^{EGFP} cells from *P2rx7*^{-/-} mice did not differ from the WT counterpart in the expression of gut-homing receptors (CD103 and CCR9) (Annacker et al., 2005; Zabel et al., 1999) (data not shown). PPs from *Cd3e*^{-/-} mice adoptively transferred with Foxp3-expressing *P2rx7*^{-/-} cells showed a prominent increase of Tfh cells (Figure 2A). To more directly address the role of P2X7 in Tfh cells, we competitively transferred *Cd3e*^{-/-} mice with Tfh cells purified from PPs of WT (CD45.1⁺) and *P2rx7*^{-/-} (CD45.2⁺) mice at a 1:1 ratio. After 1 month, more than 90% of the Tfh cells recovered from PPs of reconstituted mice originated from *P2rx7*^{-/-} mice, indicating that *P2rx7* deletion conferred greatly enhanced reconstitution potential to Tfh cells (Figure 2B).

To exclude the possibility that the expansion of Tfh cells in *P2rx7*^{-/-} mice was driven by inheritable differences in intestinal microbiota we analyzed Tfh cells in PPs from cohoused WT and *P2rx7*^{-/-} mice, which were either delivered through caesarian and cofostered (CoF) with CD1 adoptive mothers (Figure 2C) or cross-fostered (CrF) with reciprocal WT and *P2rx7*^{-/-} mothers (Figure 2D) or cobred (CoB) with WT and *P2rx7*^{-/-} mothers (Figure 2E). In all these breeding conditions, *P2rx7*^{-/-} mice sacrificed at 8 weeks of age showed an increase in Tfh cell numbers. Finally, reconstitution of cohoused *Cd3e*^{-/-} mice with WT or *P2rx7*^{-/-} Foxp3-expressing T cells also showed the selective expansion of Tfh cell numbers in mice transferred with *P2rx7*^{-/-} cells (Figure 2A). Taken together, these results demonstrate that expansion of Tfh cell numbers is T cell intrinsic and not secondary to inheritable dysbiosis in *P2rx7*^{-/-} mice.

P2X7 Mediates Tfh Cell Death

We analyzed PPs from WT and *P2rx7*^{-/-} mice by terminal deoxynucleotidyl transferase dUTP nick end labeling (TUNEL). This assay revealed the reduction of positive cells in *P2rx7*^{-/-} mice (Figure 3A). Because P2X7-mediated cell death is characterized by phosphatidylserine (PS) exposure, we analyzed PP cells for Annexin V staining by flow cytometry; more than 20% of ex vivo Tfh cells were labeled by Annexin V in WT but not *P2rx7*^{-/-} mice, whereas Annexin V staining in other PP cell subsets was consistently lower and indistinguishable between the two strains (Figure 3B). These results indicate that P2X7 expression correlates with selective Tfh cell death in PPs.

In peripheral lymph nodes and spleen of nonimmunized animals, Tfh cells are virtually absent, and *P2rx7*^{-/-} mice did not show differences with respect to WT animals (Figure S2A). In contrast, Tfh cells could be detected in mesenteric lymph nodes (mLNs) because of constant antigenic challenge. As observed in PPs, significant increases in Annexin V⁺ Tfh cells were detected in mLNs from WT mice, suggesting that P2X7 also regulates Tfh cell representation in LNs (Figure S2B; Wilhelm et al., 2010). The increase in cell death of PP Tfh cells in WT mice was confirmed with VAD-FMK staining detecting activated caspases and by increased expression of proapoptotic *bik* (Boyd et al., 1995) and *bax* (Oltvai et al., 1993) transcripts (Figure S2C). An analogous result together with selective increase in Annexin V⁺ Tfh cells was obtained with converted WT but not *P2rx7*^{-/-} Tfh cells in adoptively transferred *Cd3e*^{-/-} mice (Figure S2D), indicating the cell-autonomous nature of P2X7-mediated Tfh cell death. This conclusion was further supported by the significant increase of Annexin V⁺ cells in *Cd3e*^{-/-} mice reconstituted with Tfh cells purified from PPs of WT mice (Figure S2E).

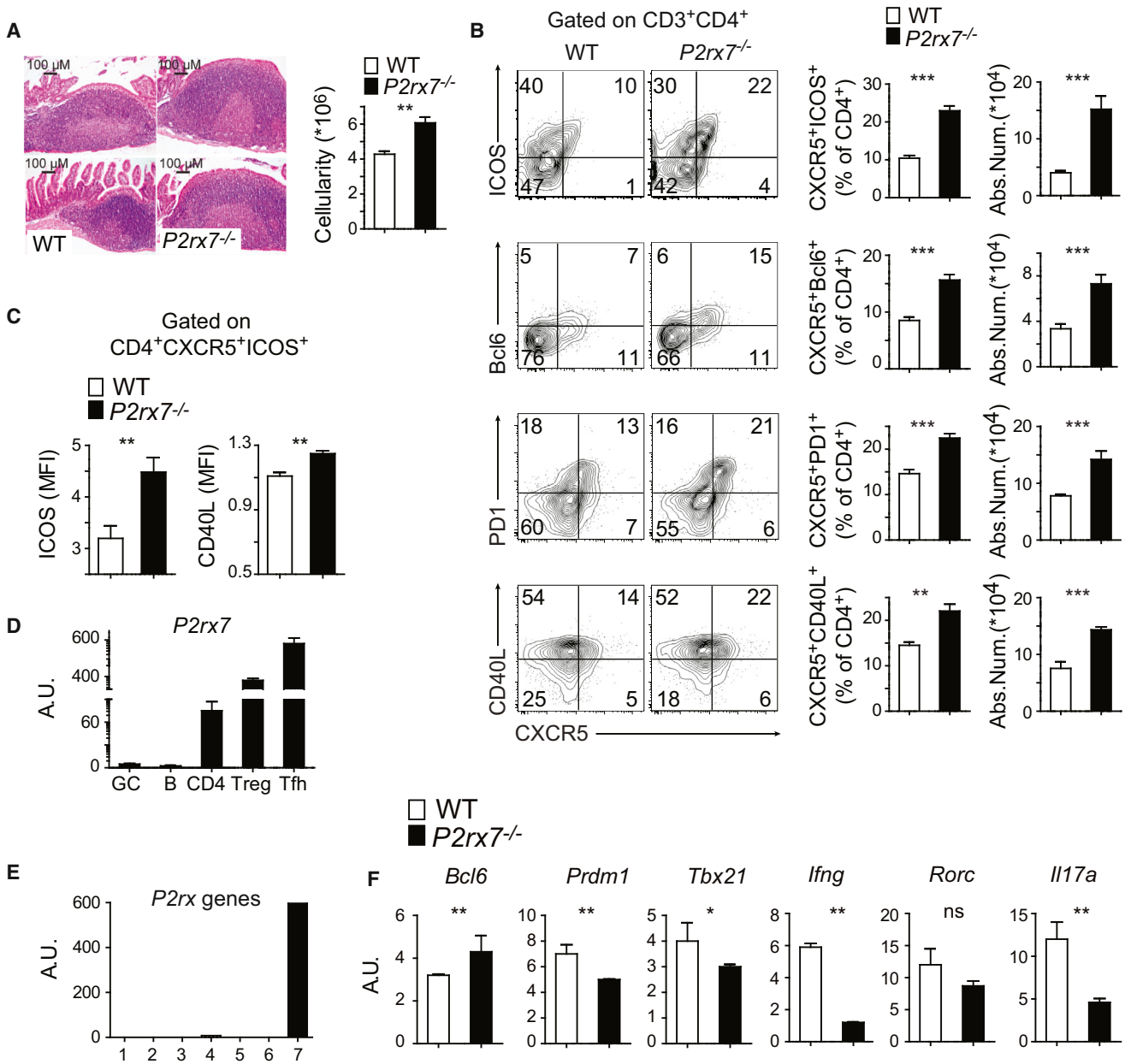


Figure 1. *P2rx7*^{-/-} Mice Have Increased Tfh Cell Numbers in the PP

(A) Ileal PPs from 8-week-old mice (scale bars represent 100 μ m); histograms show the number of total cells (mean \pm SD, n = 5) recovered from PPs harvested from the entire small intestine.

(B) Dot plot and statistical analyses of WT and *P2rx7*^{-/-} CD3⁺CD4⁺ PPs cells stained with ICOS, Bcl6, PD1, CD40L, and CXCR5 antibodies. Percentages are shown in each gate, histograms show mean percentages \pm SD (n = 5).

(C) Mean fluorescence intensity (MFI) of ICOS and CD40L on Tfh cells from WT or *P2rx7*^{-/-} quantified by flow cytometry.

(D) Quantitative real-time PCR of *P2rx7* transcripts in purified CD19⁺B220⁺, Fas⁺PNA⁺ GC B cells, CD19⁺ B cells, CD3⁺CD4⁺ T cells, CD3⁺CD4⁺CD25^{hi} Treg cells, and CD3⁺CD4⁺CXCR5⁺ICOS⁺ Tfh cells from WT mice.

(E) Quantitative real-time PCR of *P2rx* gene transcripts in purified CD3⁺CD4⁺CXCR5⁺ICOS⁺ Tfh cells from WT mice.

(F) Quantitative real-time PCR of *Bcl6*, *Prdm1*, *Tbx21*, *Ifng*, *Rorc*, and *Il17a* transcripts in purified CD3⁺CD4⁺CXCR5⁺ICOS⁺ Tfh cells from WT or *P2rx7*^{-/-} mice. Data are representative results of three independent experiments with at least five mice per experiment. *p < 0.05, **p < 0.01, and ***p < 0.001; ns, not significant. Error bars represent SD.

Analysis of permeability to DAPI upon stimulation with the P2X7 agonist BzATP showed that Tfh cells were the most sensitive subset to P2X7-mediated pore formation in PPs (Figure 3C).

Time monitoring of PS exposure and DAPI uptake upon P2X7 stimulation using the natural ligand ATP confirmed the lack of PS exposure and DAPI uptake in *P2rx7*^{-/-} Tfh cells (Figure 3D).

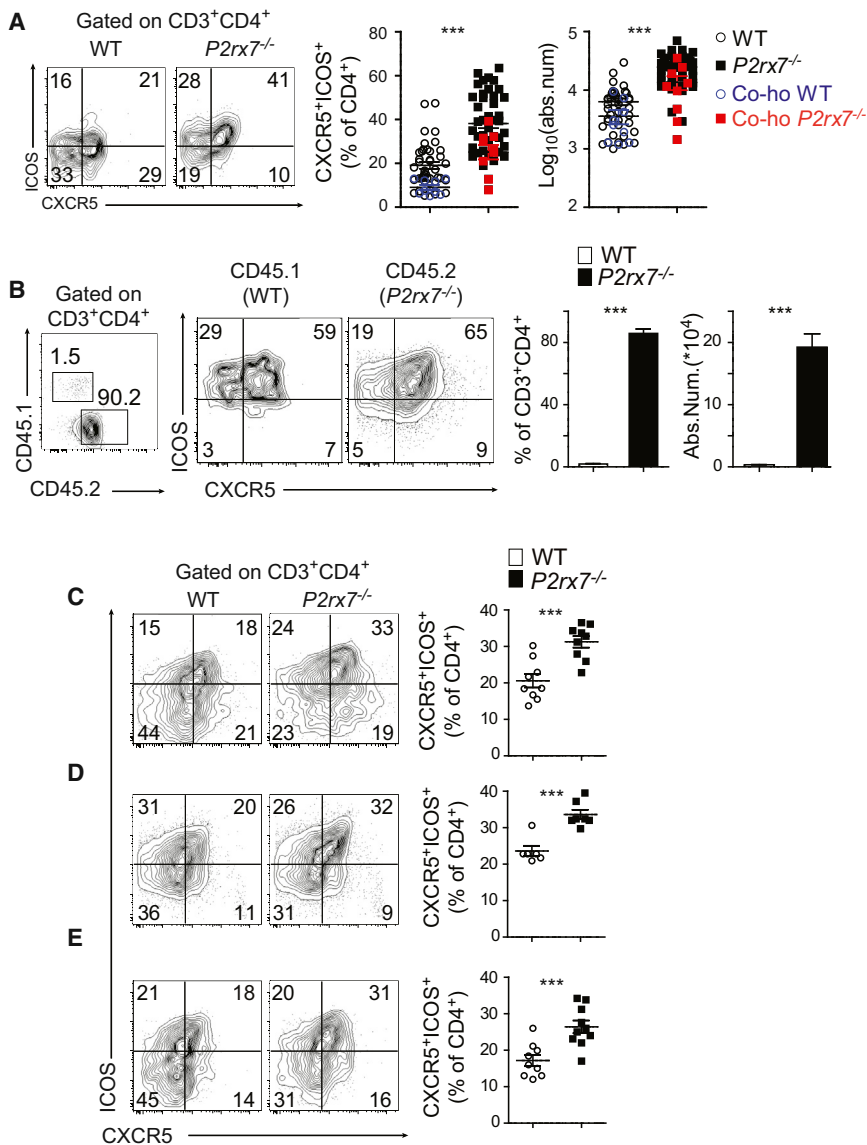


Figure 2. Expansion of Tfh Cell Numbers in the PPs of *P2rx7*^{-/-} Mice Is Cell Autonomous

(A) Dot plot and statistical analyses of PPs cells from *Cd3e*^{-/-} mice reconstituted with WT or *P2rx7*^{-/-} Foxp3^{EGFP} cells. In two independent experiments, cohoused *Cd3e*^{-/-} mice were analyzed 4 weeks after the reconstitution and are shown as superimposed blue and red results for mice reconstituted with WT or *P2rx7*^{-/-} Foxp3^{EGFP} cells, respectively.

(B) Dot plot and statistical analyses of PPs cells from *Cd3e*^{-/-} mice reconstituted with purified WT (CD45.1) and *P2rx7*^{-/-} (CD45.2) Tfh cells at 1:1 ratio. Cells were gated for surface CD4 and CD3, and ICOS⁺CXCR5⁺ cells were analyzed for CD45.1 and CD45.2 to score WT and *P2rx7*^{-/-} cells (left dot plot). Middle panels show staining with CXCR5 and ICOS antibodies on gated WT and *P2rx7*^{-/-} CD4 cells. Histograms on the right show statistics for percentage and absolute cell number of WT and *P2rx7*^{-/-} Tfh cells recovered from PPs of reconstituted *Cd3e*^{-/-} mice (n = 3).

(C–E) Flow cytometry of PPs CD3⁺CD4⁺ T cells stained with CXCR5 and ICOS antibodies; cells were recovered from cohoused WT and *P2rx7*^{-/-} mice. Before cohousing, mice were delivered through caesarean and cofostered with CD1 adoptive mothers (C), cross-fostered with reciprocal WT and *P2rx7*^{-/-} mothers and cohoused for 4 weeks (D), or cobred with WT and *P2rx7*^{-/-} mothers and cohoused for 4 weeks (E).

Data are representative results of six (A), two (B), and three (C–E) independent experiments with three to five mice per experiment. ***p < 0.001. Error bars represent SD.

P2X7 in Tfh Cells Limits GC Reaction in PPs

The increase of Tfh cells in *P2rx7*^{-/-} mice correlated with an enhanced GC reaction in the PPs (Figure 4A); the increase in Fas⁺PNA⁺ GC B cells was associated with increased expression of *Aicda*

mRNA encoding activation-induced cytidine deaminase (AID), which controls Ig somatic hypermutation (SHM) and class switch recombination (CSR) (Figure 4B; Muramatsu et al., 2000). In vitro stimulation of both T and B cells results in extracellular ATP release (Scheda et al., 2013; Schenk et al., 2008). To see whether P2X7 activation affected Tfh cell activity in vitro, WT IgM⁺ B cells were cocultured with either WT or *P2rx7*^{-/-} Tfh cells isolated from PPs; when *P2rx7*^{-/-} Tfh cells were present in the culture, there was increased Ig CSR to IgA with more abundant IgA secretion, suggesting that lack of P2X7 results in enhanced B cell helper function (Figure 4H). The number of IgA-secreting B cells measured by ELISPOT was significantly increased in the small but not large intestine lamina propria of *P2rx7*^{-/-} mice, consistent with increased Tfh cell activity in vivo (Figure 4C). Accordingly, fecal IgA concentrations in *P2rx7*^{-/-} mice were elevated, whereas IgM were reduced (Figure 4D). The same phenotype was observed in *Cd3e*^{-/-} mice reconstituted with *P2rx7*^{-/-} Foxp3⁺ T cells, indicating the dependence of

Analogous sensitivity to ATP stimulation was observed in Tfh cells from WT but not *P2rx7*^{-/-} mLN (Figure S2F), indicating that Tfh cells are exquisitely sensitive to P2X7-mediated cell death by extracellular ATP.

Importantly, extracellular ATP-mediated Tfh cell death via P2X7 does not affect Tfh cells actively responding to cognate antigen stimulation. Indeed, *p2rx7* transcription in Tfh cells was robustly downregulated by CD3 and CD28 stimulation and Tfh cells became resistant to P2X7-mediated DAPI permeability (Figure 3E). Further, we generated antigen-specific Tfh cells by feeding TCR transgenic OT-II mice (recognizing OVA peptide 323–339) with OVA. After 7 days we analyzed the amount of *P2rx7* transcripts in ex vivo sorted OT-II Tfh cells from PPs as well as in OT-II Tfh cells sorted after in vitro stimulation for 16 hr with dendritic cells pulsed with OVA peptide. This analysis revealed the robust *P2rx7* downregulation in antigen-stimulated cells (Figure 3F), thereby supporting the notion that acute TCR stimulation spares Tfh cells from death via P2X7.

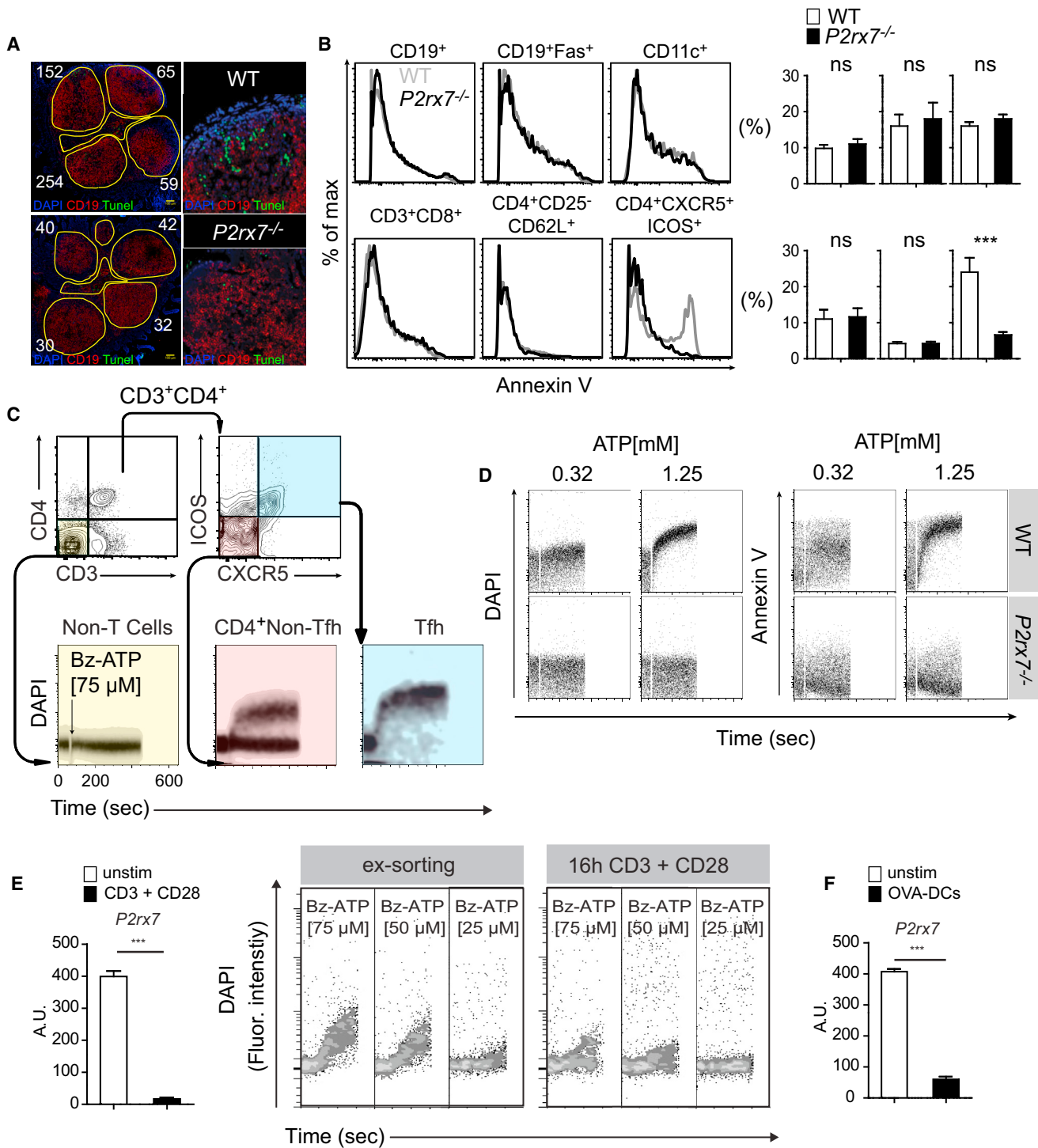


Figure 3. Extracellular ATP Promotes Tfh Cell Death

(A) Representative TUNEL assay on ileal PPs from WT and *P2rx7*^{-/-} mice (scale bars represent 100 μm); white numbers represent TUNEL-positive cells. (B) Annexin V staining and corresponding statistical analysis of freshly isolated WT and *P2rx7*^{-/-} PP cell subsets gated as indicated (n = 5). (C) Time monitoring of electronically gated PP cell subsets for DAPI uptake after stimulation with Bz-ATP (75 μM). (D) Time monitoring of electronically gated PP WT or *P2rx7*^{-/-} Tfh cells for DAPI uptake and PS exposure after stimulation with the indicated doses of ATP. (E) Real-time PCR of *P2rx7* transcripts in Tfh cells either unstimulated or stimulated for 16 hr with anti-CD3 and CD28 mAbs; Bz-ATP responsiveness measured by time-monitoring of DAPI staining in the same cells. (F) Real-time PCR of *P2rx7* transcripts in OT-II Tfh cells either unstimulated or stimulated for 16 hr with OVA peptide-pulsed dendritic cells. Data are representative results of three to six independent experiments. ***p < 0.001; ns, not significant. Error bars represent SD.

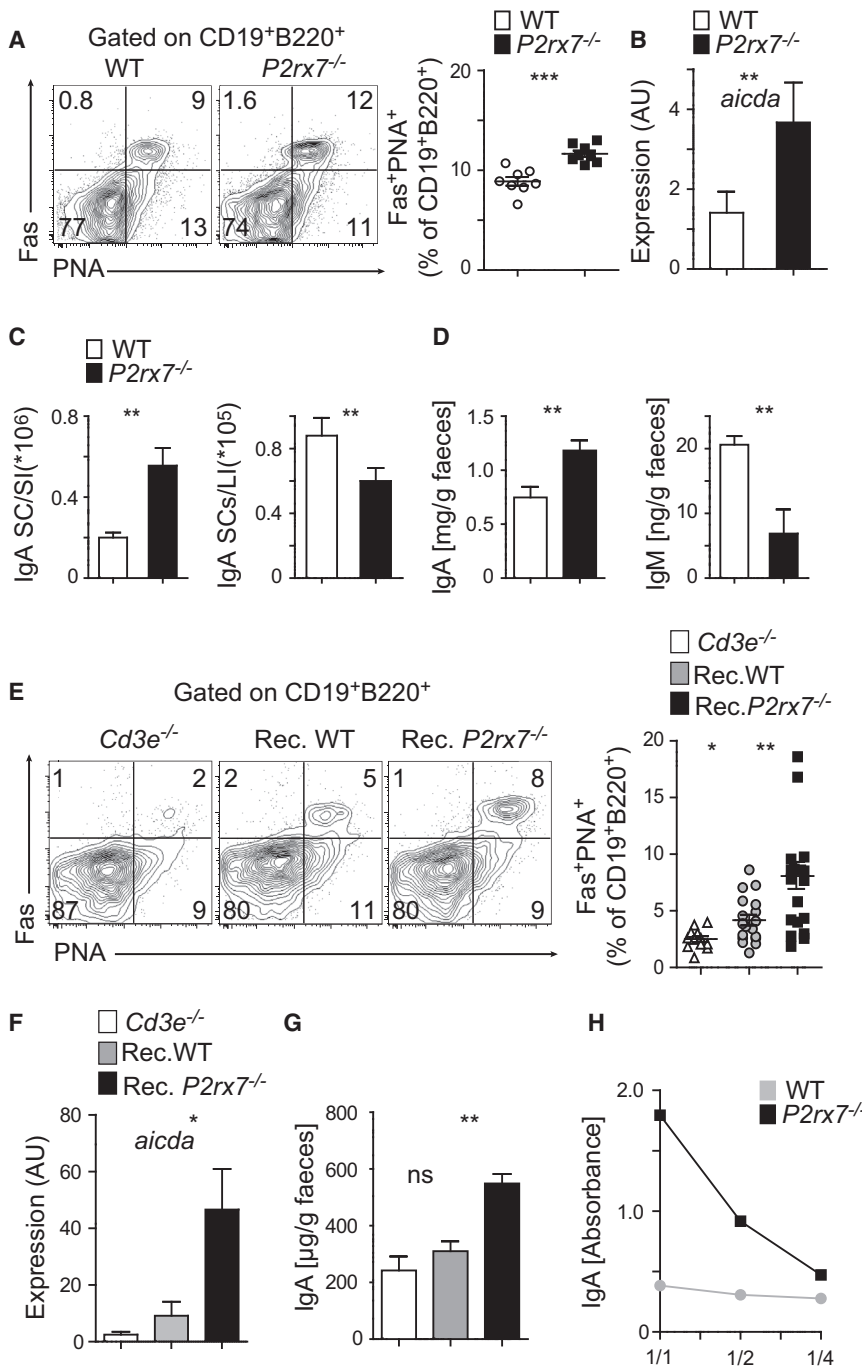


Figure 4. P2X7 Deficiency in Tfh Cells Leads to Enhanced GC Reactions and IgA Response

(A) Representative dot plots and statistical analysis of Fas⁺PNA⁺ GC B cells. (B) Real-time PCR of *Aicda* in purified CD19⁺ cells (n = 5). (C) IgA-secreting plasma cells in lamina propria of small (SI) or large (LI) intestine quantified by ELISPOT (n = 3). (D) Fecal IgA (n = 10) and IgM (n = 5) concentrations in WT and *P2rx7*^{-/-} mice. (E–G) Representative dot plots and statistical analysis of Fas⁺PNA⁺ GC B cells (E), real-time PCR of *Aicda* in purified CD19⁺ cells (n = 5) (F), and fecal IgA concentrations (n = 6) (G) in *Cd3e*^{-/-} mice either nonreconstituted or reconstituted with WT or *P2rx7*^{-/-} Foxp3^{EGFP} cells. (H) Absorbance values in ELISA-detecting IgA in the supernatants of B cells cocultured with WT or *P2rx7*^{-/-} Tfh cells purified from PPs. Data are representative results of at least two independent experiments. *p < 0.05, **p < 0.01, and ***p < 0.001; ns, not significant. Error bars represent SD.

Wild-type Tfr cells were more resistant to cell death than Tfh cells, as determined by cell labeling with Annexin V (Figure S3C). Interestingly, in Tfr cells we observed increased surface expression of the plasma membrane ectonucleotidase CD39 (that degrades ATP to ADP/AMP) with respect to Tfh cells, likely reducing P2X7 sensitivity to extracellular ATP (Figure S3D). These observations suggest that *P2rx7* deletion does not influence Tfr cells. In mice reconstituted with Foxp3⁺ cells, we observed more than 90% conversion of *P2rx7*^{-/-} Treg to Tfh cells in PPs. *P2rx7*^{-/-} Treg cells converted to Tfh cells more efficiently than WT Treg cells (Figure S3E), suggesting that lack of P2X7 results in skewing and/or expansion of Tfh but not Tfr cells. Finally, transfer into *Cd3e*^{-/-} mice of CD4⁺CXCR5⁺ICOS⁺ cells, comprising both Tfh and Tfr cells, resulted in the recovery of mostly CD4⁺CXCR5⁺ICOS⁺Foxp3⁻ Tfh cells after 4 weeks (Figure S3F), indicating that lack of P2X7 does not result in Tfr cell expansion.

the observed phenotype on *P2rx7* deletion in Tfh cells (Figures 4E–4G).

Follicular regulatory (CD4⁺CXCR5⁺ICOS⁺Foxp3⁺) T (Tfr) cells play a crucial role in GC responses by limiting Tfh and GC B cell numbers as well as plasma cells differentiation (Chung et al., 2011; Linterman et al., 2011; Wollenberg et al., 2011). Because *P2rx7* is expressed in Tfr cells (Figure S3A), *P2rx7* deletion might result in increasing Tfr cells in PPs. However, similar Tfr cell numbers were found in WT and *P2rx7*^{-/-} mice, while the percentage was reduced in *p2rx7*^{-/-} mice (Figure S3B).

P2X7 Signaling Regulates Human Tfh Cells

TUNEL-positive cells were observed in the T cell area of human PPs (Figure 5A) as well as selective PS exposure by FACS in Tfh cells from PPs of three healthy subjects (Figure 5B). On-line monitoring of Annexin V staining and DAPI permeability of PP cells exposed to ATP revealed an increase in Tfh but not other PP cells (Figure 5C). Indeed, naive B cells do not express

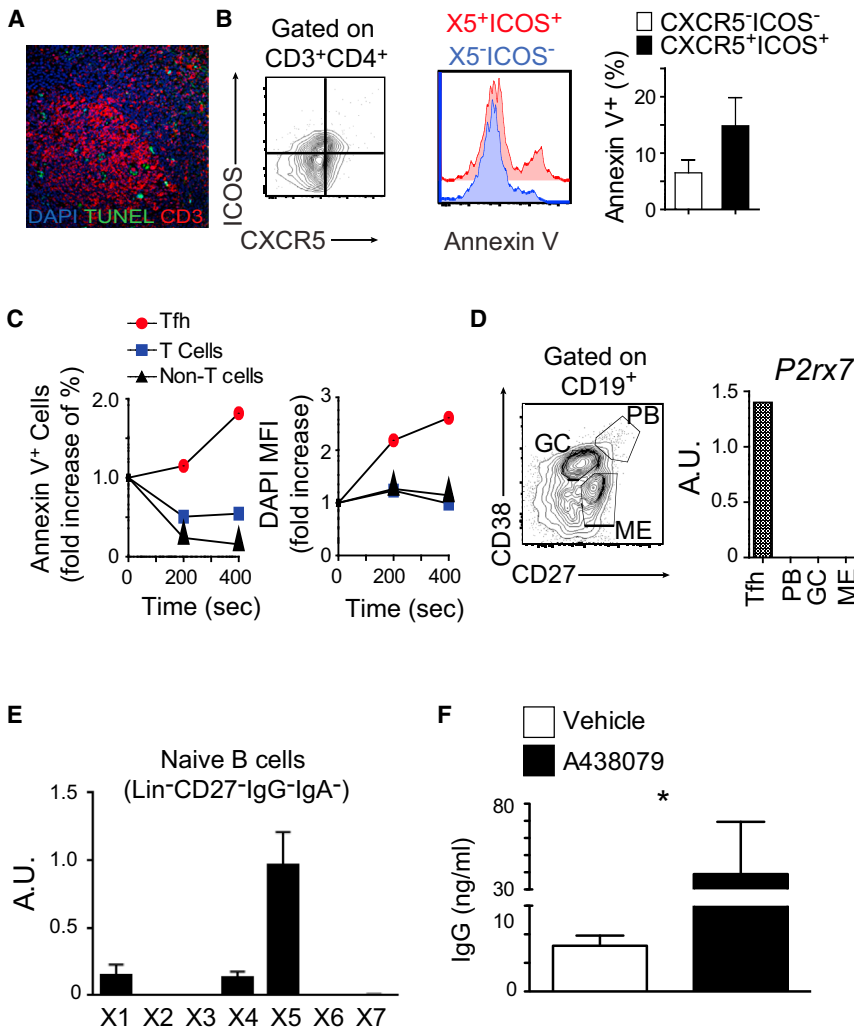


Figure 5. Purinergic Regulation of Tfh Cells Is Conserved in Humans

(A) Representative TUNEL assay on ileal PPs from a healthy subject.

(B) Cell suspensions from human PPs were stained with CD3, CD4, CXCR5, and ICOS antibodies. A representative staining with Annexin V of CD3⁺CD4⁺ICOS⁻CXCR5⁻ (X5⁻ICOS⁻) and Tfh (X5⁺ICOS⁺) cells is shown. Bars on the right show statistical analysis of Annexin V staining for three subjects.

(C) Fold increase of Annexin V⁺ cells and DAPI MFI in the indicated cell subsets recovered from PPs of healthy subject upon stimulation with 3 mM ATP.

(D) Gating strategy for purification of the indicated cell subsets and real-time PCR of *P2rx7* transcripts in germinal center B cells (GC), plasmablasts (PB), memory B (ME), and Tfh cells purified in flow cytometry from ileal PPs of healthy subjects.

(E) Real-time PCR of *P2rx7* transcripts in naive B cells sorted as CD19⁺IgM⁺IgD⁺CD27⁻ from blood of three healthy donors.

(F) Quantification of IgG by ELISA in the supernatants of blood naive B cells cultured with purified memory CXCR5⁺CD45RA⁻CD4⁺ T cells in presence of P2X7 antagonist (A438079).

Results are means ± SD of five independent experiments with cells from five different healthy donors. *p < 0.05. Error bars represent SD.

detectable amounts of *P2rx7* (Figure 5E), and *P2rx7* transcripts were not detected in plasma blasts (PBs), GC, and memory (ME) B cells by real-time PCR (Figure 5D). These observations suggest that luminal ATP can also modulate Tfh cell function in the human small intestine. To address the role of P2X7 in regulating B cell help by Tfh cells, an in vitro assay of Ig CSR was performed in the presence of a selective P2X7 pharmacological antagonist (A438079). Naive B cells isolated from peripheral blood as CD19⁺Lin⁻CD27⁻IgG⁻IgA⁻ cells predominantly express *P2rx5* and to a lesser extent *P2rx1* and *P2rx4* (Figure 5E), and therefore they were not directly influenced by the drug. Coculturing of naive B cells with Tfh cells isolated from peripheral blood as CD4⁺CXCR5⁺CD45RA⁻ cells (Morita et al., 2011) resulted in substantial Ig CSR to IgG. Notably, inhibition of P2X7 by A438079 resulted in an increase of IgG concentration in the culture medium (Figure 5F), suggesting that P2X7 activity is also important for regulating human Tfh cells.

***P2rx7*^{-/-} Mice Have Enhanced High-Affinity IgA Responses and Reduced Mucosal Colonization**

Mucosal IgA inhibits intestinal bacteria from penetrating the epithelial cell layer (Burns et al., 1996; Macpherson and Uhr,

epithelial cells in the terminal ileum (Ivanov et al., 2009; Suzuki et al., 2004). High-throughput sequencing of Ig V_H regions in B cells isolated from PPs revealed minor differences between WT and *P2rx7*^{-/-} mice in the distribution of the V_H repertoire of IgA (Figure 6A). However, an increase in the frequency of replacement (R) mutations (i.e., encoding a different amino acid) in V_{H1} family's CDR2 was detected in *P2rx7*^{-/-} mice, suggesting enhanced affinity maturation of IgA responses (Figure 6B). Analysis in flow cytometry of IgA-coated bacteria from the small intestine revealed the increase of IgA-coated cells in *P2rx7*^{-/-} mice. Conversely, bacteria coated by IgG₃, a T-cell-independent Ig subclass present in the small intestine and specific for bacterial polysaccharides (McLay et al., 2002), were the same for both strains (Figure 6C). Inspection of the ileum from WT and *P2rx7*^{-/-} mice by scanning electron microscopy (SEM) revealed the striking reduction of mucosal colonization by SFB in *P2rx7*^{-/-} mice (Figure 6D). To demonstrate enhanced high-affinity IgA responses in *P2rx7*^{-/-} mice, we gavaged mice with *E. coli* and analyzed the specific IgA response. In fact, the *E. coli*-specific IgA response is fully dependent on PPs (Lécuyer et al., 2014). Total IgA concentration in intestinal washes was quantified by ELISA. Undiluted aliquots of the

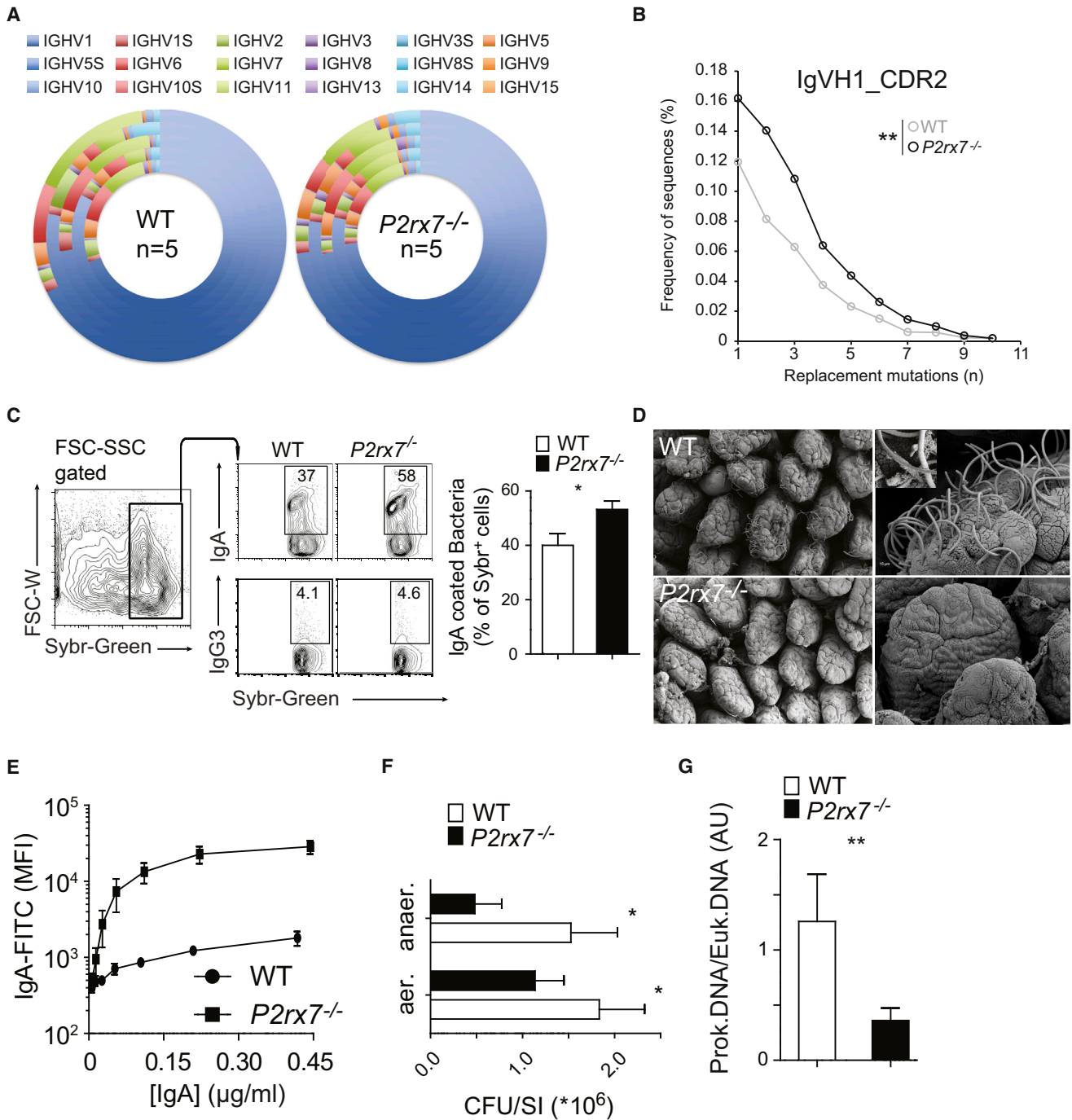


Figure 6. P2X7 Deficiency Leads to Enhanced IgA Affinity and Depletion of Mucosal Commensals

(A and B) V_H family distribution in five mice per genotype (A) and frequency of R mutations in IgV_{H1} family CDR2 (B) in IgA-expressing CD19⁺ B cells isolated from PPs of WT and P2rx7^{-/-} mice.

(C) Representative dot plots and percentages of IgA (n = 6)- and IgG₃ (n = 6)-coated bacteria from the small intestine of WT and P2rx7^{-/-} mice as determined by flow cytometry.

(D) SEM of the terminal ileum from WT and P2rx7^{-/-} mice. Inset in WT image shows SFBs in more detail.

(E) Quantification by flow cytometry of *E. coli*-specific IgA in intestinal lavages from WT and P2rx7^{-/-} mice gavaged with *E. coli*.

(F) Statistical analysis of colony forming units (CFU) of aerobic and anaerobic bacteria recovered from the SI of WT and P2rx7^{-/-} mice (n = 10).

(G) Quantitative real-time PCR of ileal adherent bacteria in WT and P2rx7^{-/-} mice expressed as prokaryotic/eukaryotic DNA ratio (n = 5).

Data are from one experiment (A and B) or at least two independent experiments. *p < 0.05, **p < 0.01. Error bars represent SD.

same samples were used to stain *E. coli* for FACS analysis. Mean fluorescence intensities of *E. coli*-specific IgA plotted against IgA concentrations revealed an increase of *E. coli*-specific IgA in $P2rx7^{-/-}$ mice, thereby indicating that PP-dependent IgA response was enhanced (Figure 6E). Taxonomic analysis of total gut microbiota in WT and $P2rx7^{-/-}$ mice did not reveal differences in the representation of bacterial families (Figure S4A). However, bacterial cultures from small intestine of $P2rx7^{-/-}$ mice showed a decrease of both aerobic and anaerobic species (Figure 6F). Finally, after removal of fecal pellet, we isolated whole ileal mucosa comprising epithelium and mucus (Figure S4B) to quantify adherent bacteria per tissue mass by real-time PCR. In $P2rx7^{-/-}$ mice we could detect a decreased prokaryotic to eukaryotic DNA ratio (Figure 6G), indicating that P2X7 in Tfh cells is important in dampening high-affinity IgA responses in the small intestine and that $P2rx7$ deletion results in an enhanced clearance of mucosal commensals in the small intestine.

$P2rx7^{-/-}$ Mice Have Reduced Serum IgM and Are Susceptible to Sepsis

Sensing of commensals profoundly shapes host immune system (Hand et al., 2012; Hooper et al., 2012). In $P2rx7^{-/-}$ mice, reduced IgM serum concentrations were observed in comparison with WT animals (Figure 7A). In WT mice, long-term dosing of antibiotics resulted in reduction of serum IgM, consistent with a requirement for mucosal colonization in maintaining serum IgM at physiological concentrations (Figure 7A). It was recently found that lack of IgA negatively correlates with serum lipopolysaccharide (LPS) concentrations (Shulzhenko et al., 2011). Hyper-IgA in $P2rx7^{-/-}$ mice was associated with reduced concentrations of serum LPS (Figure 7B). In addition, a single low-dose (20 μ g) intraperitoneal injection of LPS induced a significant increase in serological IgM in $P2rx7^{-/-}$ mice (Figure 7C), suggesting that reduced mucosal colonization and consequently less translocation of bacterial components results in reduced B cell stimulation and IgM secretion.

Because deletion of *Icos* results in a lack of Tfh cells in both P2X7-proficient and P2X7-deficient mice (Figure S5A), we used *Icos*^{-/-} and double mutant *Icos*^{-/-} $P2rx7^{-/-}$ mice to address the role of P2X7 in Tfh cells for conditioning serum IgM concentrations through the regulation of mucosal IgA. By comparing the ratio of $P2rx7^{-/-}$ to $P2rx7^{+/+}$ fecal IgA and serum IgM in ICOS-proficient and ICOS-deficient mice, we found that *Icos* deletion restored the balance between fecal IgA and serum IgM in $P2rx7^{-/-}$ mice (Figure 7D). These results suggest that Tfh cells are responsible for the elevated fecal IgA and reduced serum IgM characteristic of $P2rx7^{-/-}$ mice.

Evaluation of IgM-secreting cells (ISCs) in the spleen by ELISPOT assay revealed the decrease of ISCs in $P2rx7^{-/-}$ mice with respect to their WT counterpart. ISCs reduction in $P2rx7^{-/-}$ mice was Tfh cell dependent since it was restored by *Icos* deletion (Figure S5B). Further investigation of the spleens of $P2rx7^{-/-}$ mice revealed that follicular and marginal zone B cells were not able to spontaneously secrete IgM (data not shown) whereas B1 cells did and were responsive to stimulation by commensals components. In fact, IgM secretion by these cells was reduced in germ-free mice and was restored in $P2rx7^{-/-}$ mice by LPS injection (Figures 7E and 7F).

Serum from $P2rx7^{-/-}$ mice (1:4 dilution) showed reduced IgM binding to antigens from cecal commensals compared to serum from WT mice (Figure 7G) as well as impaired ability to inhibit cecal bacteria growth in vitro (Figure 7H). Notably, this serological defect of $P2rx7^{-/-}$ mice was restored by addition of purified IgM from the sera of WT mice (Figure 7H), suggesting that translocation of bacterial antigens from the small intestine results in the priming of B cells to secrete IgM able to inhibit bacterial growth and that this priming is significantly defective in $P2rx7^{-/-}$ mice.

It is known that IgM constitutes a first line of defense against blood-borne microbial infection (Boes et al., 1998), and thus the reduced concentrations of IgM in $P2rx7^{-/-}$ mice should make them more susceptible to polymicrobial sepsis. To test this hypothesis, a sublethal terminal cecal ligation and puncture (CLP) was performed. This model has been shown to closely resemble human sepsis (Hubbard et al., 2005; Rittirsch et al., 2009). Strikingly, $P2rx7^{-/-}$ mice displayed severe symptoms in the first hours after surgery and most succumbed within 48 hr (Figures 7I and 7L). Although blood from WT mice was always sterile, both aerobic and anaerobic bacteria could be easily cultured from blood of $P2rx7^{-/-}$ mice (Figure S5C). The same morbidity was observed by CLP in cohoused WT and $P2rx7^{-/-}$ mice, suggesting that lack of P2X7 results in the depletion of “protective” commensals (Figure S5D). Notably, $P2rx7^{-/-}$ mice surviving CLP showed an increase of serological IgM concentrations relative to WT mice, indicating that $P2rx7^{-/-}$ B cells were not intrinsically defective in differentiating to ISCs upon stimulation by bacterial antigens (Figure 7M). Prophylactic intravenous affinity-purified IgM from WT mice was administered to $P2rx7^{-/-}$ mice before CLP. IgM-treated mice were indistinguishable from WT mice and showed comparable survival rates (Figures 7I and 7L), implicating reduced IgM as cause of mortality by polymicrobial sepsis in $P2rx7^{-/-}$ mice. Of note, infection with *Listeria monocytogenes*, in which adaptive immunity is dispensable for containing infection at early time points (Pamer, 2004), did not result in differences for morbidity and bacterial recovery between WT and $P2rx7^{-/-}$ mice (Figures S5E and S5F). To show the causative role of $P2rx7^{-/-}$ Tfh cells in bacterial sepsis after sublethal CLP, the same experiment was repeated in $P2rx7^{-/-}$ *Icos*^{-/-} mice. Strikingly, these mice were fully resistant to sublethal CLP, analogously to *Icos*^{-/-} animals (Figure S7N). These results indicate that enhanced adaptive mucosal response in $P2rx7^{-/-}$ mice attenuates systemic sensing and basal IgM response to commensals, thus exposing the organism to possible fatal sepsis.

DISCUSSION

The regulated release of ATP influences eukaryotic cell function through ubiquitously expressed purinergic P2 receptors (Burnstock, 2007). The high concentration of ATP inside cells and its virtual absence extracellularly in healthy tissues renders ATP also an ideal harbinger of cell death; in fact, ATP is sensed as a DAMP by cells of the innate immune system. $P2rx7$ has been recently shown to be a signature gene of Tfh cells (Choi et al., 2013; Iyer et al., 2013), but its function in this cell subset has not been addressed so far. Interestingly, extracellular ATP concentrations active on P2X7 are present during an alloreactive response and at site of immunization with complete Freund's

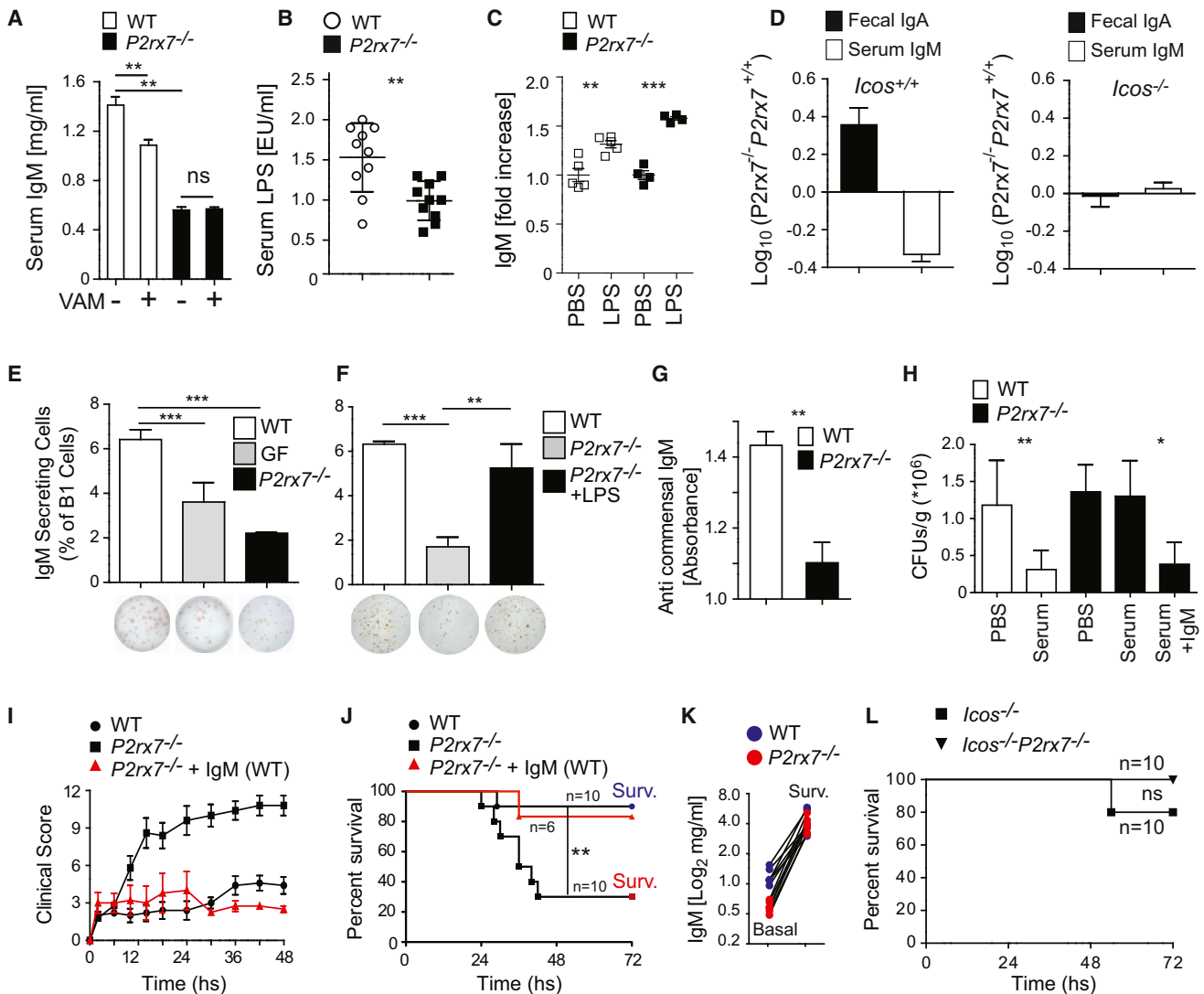


Figure 7. P2X7 Deficiency Is Associated with Reduced IgM-Secreting B1 Cells and Susceptibility to Polymicrobial Sepsis

(A) ELISA quantification of serum IgM in WT and *P2rx7*^{-/-} mice treated either with PBS (-) or VAM (+) (n = 3).
 (B) Serum LPS concentrations in WT and *P2rx7*^{-/-} mice as determined by *Limulus* amoebocyte lysate (LAL) assay.
 (C) ELISA quantification of serum IgM concentrations in WT and *P2rx7*^{-/-} mice treated either with PBS or LPS.
 (D) Ratio of *P2rx7*^{-/-} to *P2rx7*^{+/+} fecal IgA (n = 10) and serum IgM (n = 6) in *Icos*^{+/+} (left) and *Icos*^{-/-} (right) backgrounds.
 (E) Representative picture and mean percentages of IgM-secreting cells by ELISPOT in purified splenic B1 cells from WT, germ-free (GF), and *P2rx7*^{-/-} mice (WT, 20 mice pooled in group of 5; GF, 10 mice pooled in group of 5; *P2rx7*^{-/-}, 15 mice pooled in group of 5).
 (F) Representative picture and mean percentages of IgM-secreting cells by ELISPOT in purified splenic B1 cells from WT, *P2rx7*^{-/-}, and *P2rx7*^{-/-} mice treated with intraperitoneal injection of LPS (WT, 10 mice pooled in group of 5; *p2rx7*^{-/-}, 10 mice pooled in group of 5; *p2rx7*^{-/-} treated with LPS, 10 mice pooled in group of 5).
 (G) Absorbance in ELISA of antimicrobiota serum IgM in WT and *P2rx7*^{-/-} mice (n = 5).
 (H) CFUs in cecal cultures from WT and *P2rx7*^{-/-} mice with addition of PBS or autologous serum and IgM from WT mice (serum + IgM) (n = 5).
 (I and J) Clinical score (I) and survival rate (J) of WT, *P2rx7*^{-/-}, and *P2rx7*^{-/-} mice treated with IgM purified from WT mice, upon sublethal CLP.
 (K) Serum IgM concentrations by ELISA in surviving WT and *P2rx7*^{-/-} mice before and 1 week after CLP.
 (L) Survival rates of *Icos*^{-/-} and *P2rx7*^{-/-}*Icos*^{-/-} mice upon sublethal CLP.
 Data are representative results of two to five independent experiments. *p < 0.05, **p < 0.01, and ***p < 0.001. Error bars represent SD.

adjuvant (Wilhelm et al., 2010), suggesting that signaling through the ATP-P2X7 axis can regulate Tfh cell response in secondary lymphoid organs.

Tfh-cell-dependent high-affinity IgA is critical in maintaining intestinal homeostasis and efficient mucosal defense by limiting translocation of potentially invasive bacteria from the

gut lumen into the organism (Wei et al., 2011; Shroff et al., 1995). Conversely, microbiota-independent (“natural”) and T-cell-independent (“primitive”) IgA are sufficient for controlling benign commensal bacteria by promoting their exclusion from the mucus layer (Slack et al., 2012). In an elegant study, Hapfelmeier et al. (2010) have shown that mucosal IgA response in the

gut is adapted to actual commensals. In Tfh cells, *P2rx7* is robustly downregulated by acute TCR stimulation, thereby sparing actively responding cells from death via P2X7. The sensitivity of non-actively stimulated Tfh cells to ATP as a metabolite associated with mucosal colonization might underlie IgA attrition in the gut and allow adapting IgA response to predominant taxa at any given time. Probably this mechanism contributes also to the complexity of developing vaccines that effectively protect the host against intestinal mucosal infections (Slack et al., 2012). Notably, oral immunization of *P2rx7*^{-/-} mice with *E. coli* resulted in dramatically enhanced IgA response with respect to WT mice. Because Tfh cell death by extracellular ATP was observed also in human PPs, pharmacological ATP antagonism might constitute a strategy to limit Tfh cells death and promote long-lasting mucosal IgA responses.

Lack of the inhibitory coreceptor PD1 was recently shown to result in expanded Tfh cells in PPs. However, the increased help by PD1-deficient cells interfered with selection of the IgA repertoire and IgA responses were not specific for commensals (Kawamoto et al., 2012). In contrast, Tfh cells expansion by *P2rx7* deletion resulted in enhanced IgA responses to commensals and to gavaged *E. coli*. Further, *P2rx7*^{-/-} mice showed increased IgA SHMs and reduced mucosal colonization, indicating enhanced antigen-specific Tfh cell help and the fact that P2X7 activity contributes to mucosal commensalism by limiting follicular T cell help.

Commensal-derived signals shape a number of systemic immune responses (Clarke et al., 2010; Hill et al., 2012; Macpherson and Harris, 2004; Noverr and Huffnagle, 2004). Secretory IgA limit access of antigens from the microbiota to the organism (Johansen et al., 1999; Macpherson and Uhr, 2004; Sait et al., 2007; Shulzhenko et al., 2011) and increased IgA are likely responsible of reduced stimulation of B1 cells as well as serum IgM concentrations in *P2rx7*^{-/-} mice. IgM plays a crucial role in protecting the organism against blood microbial infection (Boes et al., 1998) and contrast lethal dissemination of commensals (Kirkland et al., 2012). Sepsis is a major health problem (Hotchkiss and Karl, 2003); in hospitalized patients, antibiotic-induced changes in the intestinal microbiota can enable bacteria to invade the bloodstream (Ubeda et al., 2010). Hypo-IgM in *P2rx7*^{-/-} mice increases the risk of polymicrobial sepsis and death by otherwise sublethal CLP, an experimental model that closely resembles the human disease (Hubbard et al., 2005; Rittirsch et al., 2009). These results point to *P2rx7* in Tfh cells as a master regulator of host-microbiota mutualism. Finally, elevated ATP in the intestine, as may occur during invasion of the microbiota by intestinal pathogens or damage to the epithelium by pathogens, toxins, or injected chemicals, might modify the balance of immune responses toward a more potent innate response. Production of metabolically “expensive” and risky adaptive immunity can then be limited to persistent microorganisms that cannot be cleared by innate immunity alone.

EXPERIMENTAL PROCEDURES

Mice and In Vivo Experiments

All animal experiments were performed in accordance with the Swiss Federal Veterinary Office guidelines and authorized by the Animal Studies Committee of Cantonal Veterinary. Mice were on a C57BL/6 genetic background. C57BL/

6J, *P2rx7*^{-/-} (B6.129P2-*P2rx7*^{tm1Gab/J}), “*Foxp3*^{EGFP}” (B6.Cg-*Foxp3*^{tm2Tch/J}), *Icos*^{-/-}, and *Cd3e*^{-/-} mice were bred in specific-pathogen-free (spf) facility at Institute for Research in Biomedicine Switzerland. C57BL/6J germ-free mice were maintained in flexible film isolators at the Clean Animal Facility, University of Bern, Switzerland. For sublethal CLP, the cecum was ligated at 10 mm from the distal pole. Cecal puncture (“through-and-through”) in a mesenteric to antimesenteric direction was carried out after ligation with a 20G needle. Body temperature and clinical score were measured every 3 hr. Cohousing experiments were performed as follows.

For caesarean delivery and fostering by CD1 adoptive mothers (CoF), WT and *P2rx7*^{-/-} mice were delivered by caesarean section on gestation day 18.5, fed by CD1 adoptive mother, weaned at 4 weeks, cohoused, and sacrificed at 8 weeks of age. For cross-fostering with reciprocal WT and *P2rx7*^{-/-} mothers (CrF), WT mice were fed by *P2rx7*^{-/-} mother and *P2rx7*^{-/-} newborns were fed by WT mother. Cubs were weaned at 4 weeks, cohoused, and sacrificed at 8 weeks of age. For cobbreding with WT and *P2rx7*^{-/-} mothers (CoB), WT and *P2rx7*^{-/-} newborns were bred together and fed by both WT and *P2rx7*^{-/-} mothers in the same cage (up to ten cubs with two mothers). Mice were weaned at 4 weeks of age, cohoused, and sacrificed at 8 weeks of age.

Isolation of Human PPs and In Vitro Tfh-Cell-Dependent B Cell Help

Peyer’s patches were obtained during endoscopy from the terminal ileum of young adults presenting with chronic abdominal pain and in which subsequent examinations excluded the presence of organic diseases of the bowel. All patients were otherwise healthy and not taking medications. Peyer’s patches were identified at endoscopy as small nodules covered by normal mucosa. For CD4 T-B cell coculture, naive B cells were cocultured with sorted CD4⁺ T cells in the presence of endotoxin-reduced SEB. P2X7 selective antagonist A 438079 hydrochloride (Tocris) was added at a final concentration of 10 nM in the coculture. After 9 days of culture, supernatants were collected and IgG content was measured by ELISA.

Statistical Analyses

Student’s paired t test was used to determine the significance of differences between mean values. In flow cytometry analyses, mean values ± SD of at least five mice from the same experiment are shown and are representative of at least three independent experiments. Values of *p* < 0.05 were considered significant.

ACCESSION NUMBERS

The Sequence Read Archive (SRA) accession number for the Ig V_H region sequences reported in this paper is SRP049293.

SUPPLEMENTAL INFORMATION

Supplemental Information includes five figures and Supplemental Experimental Procedures and can be found with this article online at <http://dx.doi.org/10.1016/j.immuni.2014.10.010>.

AUTHOR CONTRIBUTIONS

F.G., M.P., and E.T. designed experiments. M.P. and V.C. performed most experiments. T.R.J., A.R., C.E.F., L.P., R.R., S.P., and E.T. performed experiments. E.R. contributed histochemical analysis. F.C. contributed human samples. B.B. contributed bioinformatic analysis of IgA sequencing data. M.T., K.D.M., E.S., and E.T. contributed reagents and intellectual input. F.G. and M.P. analyzed data and wrote the paper.

ACKNOWLEDGMENTS

We thank D. Jarrossay and E. Montani (Institute for Research in Biomedicine) for cell sorting and help with confocal microscopy, M. Francolini (Fondazione Filarete, Milan, Italy) for SEM, and J. Hastewell (Novartis Institute for Biomedical Research, Cambridge, MA) for comments on the manuscript. The work was supported by grant 310030-140963 and Sinergia CRSII2-127547 of the Swiss National Science Foundation, grant 2012-0519 of Fondazione Cariplo,

Nano-Tera project 20NA21-128841, Fondazione Ticinese per la Ricerca sul Cancro, Fondazione per la Ricerca sulla Trasfusione e sui Trapianti, and Converge Biotech.

Received: June 20, 2014

Accepted: October 3, 2014

Published: November 13, 2014

REFERENCES

- Adriouch, S., Dox, C., Welge, V., Seman, M., Koch-Nolte, F., and Haag, F. (2002). Cutting edge: a natural P451L mutation in the cytoplasmic domain impairs the function of the mouse P2X7 receptor. *J. Immunol.* **169**, 4108–4112.
- Annacker, O., Coombes, J.L., Malmstrom, V., Uhlig, H.H., Bourne, T., Johansson-Lindbom, B., Agace, W.W., Parker, C.M., and Powrie, F. (2005). Essential role for CD103 in the T cell-mediated regulation of experimental colitis. *J. Exp. Med.* **202**, 1051–1061.
- Boes, M., Prodeus, A.P., Schmidt, T., Carroll, M.C., and Chen, J. (1998). A critical role of natural immunoglobulin M in immediate defense against systemic bacterial infection. *J. Exp. Med.* **188**, 2381–2386.
- Boyd, J.M., Gallo, G.J., Elangovan, B., Houghton, A.B., Malstrom, S., Avery, B.J., Ebb, R.G., Subramanian, T., Chittenden, T., Lutz, R.J., et al. (1995). Bik, a novel death-inducing protein shares a distinct sequence motif with Bcl-2 family proteins and interacts with viral and cellular survival-promoting proteins. *Oncogene* **11**, 1921–1928.
- Burns, J.W., Siadat-Pajouh, M., Krishnaney, A.A., and Greenberg, H.B. (1996). Protective effect of rotavirus VP6-specific IgA monoclonal antibodies that lack neutralizing activity. *Science* **272**, 104–107.
- Burnstock, G. (2007). Purine and pyrimidine receptors. *Cell. Mol. Life Sci.* **64**, 1471–1483.
- Cerutti, A., and Rescigno, M. (2008). The biology of intestinal immunoglobulin A responses. *Immunity* **28**, 740–750.
- Choi, Y.S., Kageyama, R., Eto, D., Escobar, T.C., Johnston, R.J., Monticelli, L., Lao, C., and Crotty, S. (2011). ICOS receptor instructs T follicular helper cell versus effector cell differentiation via induction of the transcriptional repressor Bcl6. *Immunity* **34**, 932–946.
- Choi, Y.S., Yang, J.A., Yusuf, I., Johnston, R.J., Greenbaum, J., Peters, B., and Crotty, S. (2013). Bcl6 expressing follicular helper CD4 T cells are fate committed early and have the capacity to form memory. *J. Immunol.* **190**, 4014–4026.
- Chung, Y., Tanaka, S., Chu, F., Nurieva, R.I., Martinez, G.J., Rawal, S., Wang, Y.H., Lim, H., Reynolds, J.M., Zhou, X.H., et al. (2011). Follicular regulatory T cells expressing Foxp3 and Bcl-6 suppress germinal center reactions. *Nat. Med.* **17**, 983–988.
- Clarke, T.B., Davis, K.M., Lysenko, E.S., Zhou, A.Y., Yu, Y., and Weiser, J.N. (2010). Recognition of peptidoglycan from the microbiota by Nod1 enhances systemic innate immunity. *Nat. Med.* **16**, 228–231.
- Craig, S.W., and Cebra, J.J. (1971). Peyer's patches: an enriched source of precursors for IgA-producing immunocytes in the rabbit. *J. Exp. Med.* **134**, 188–200.
- Crotty, S. (2011). Follicular helper CD4 T cells (TFH). *Annu. Rev. Immunol.* **29**, 621–663.
- Förster, R., Mattis, A.E., Kremmer, E., Wolf, E., Brem, G., and Lipp, M. (1996). A putative chemokine receptor, BLR1, directs B cell migration to defined lymphoid organs and specific anatomic compartments of the spleen. *Cell* **87**, 1037–1047.
- Gavin, M.A., Rasmussen, J.P., Fontenot, J.D., Vasta, V., Manganiello, V.C., Beavo, J.A., and Rudensky, A.Y. (2007). Foxp3-dependent programme of regulatory T-cell differentiation. *Nature* **445**, 771–775.
- Hale, J.S., Youngblood, B., Latner, D.R., Mohammed, A.U., Ye, L., Akondy, R.S., Wu, T., Iyer, S.S., and Ahmed, R. (2013). Distinct memory CD4+ T cells with commitment to T follicular helper- and T helper 1-cell lineages are generated after acute viral infection. *Immunity* **38**, 805–817.
- Hand, T.W., Dos Santos, L.M., Bouladoux, N., Molloy, M.J., Pagán, A.J., Pepper, M., Maynard, C.L., Elson, C.O., 3rd, and Belkaid, Y. (2012). Acute gastrointestinal infection induces long-lived microbiota-specific T cell responses. *Science* **337**, 1553–1556.
- Hapfelmeier, S., Lawson, M.A., Slack, E., Kirundi, J.K., Stoel, M., Heikenwalder, M., Cahenzli, J., Velykoredko, Y., Balmer, M.L., Endt, K., et al. (2010). Reversible microbial colonization of germ-free mice reveals the dynamics of IgA immune responses. *Science* **328**, 1705–1709.
- Haynes, N.M., Allen, C.D., Lesley, R., Ansel, K.M., Killeen, N., and Cyster, J.G. (2007). Role of CXCR5 and CCR7 in follicular Th cell positioning and appearance of a programmed cell death gene-1high germinal center-associated subpopulation. *J. Immunol.* **179**, 5099–5108.
- Henao-Mejia, J., Elinav, E., Jin, C., Hao, L., Mehal, W.Z., Strowig, T., Thaiss, C.A., Kau, A.L., Eisenbarth, S.C., Jurczak, M.J., et al. (2012). Inflammasome-mediated dysbiosis regulates progression of NAFLD and obesity. *Nature* **482**, 179–185.
- Hill, J.A., Hall, J.A., Sun, C.M., Cai, Q., Ghyselinck, N., Chambon, P., Belkaid, Y., Mathis, D., and Benoist, C. (2008). Retinoic acid enhances Foxp3 induction indirectly by relieving inhibition from CD4+CD44hi Cells. *Immunity* **29**, 758–770.
- Hill, D.A., Siracusa, M.C., Abt, M.C., Kim, B.S., Kobuley, D., Kubo, M., Kambayashi, T., Larosa, D.F., Renner, E.D., Orange, J.S., et al. (2012). Commensal bacteria-derived signals regulate basophil hematopoiesis and allergic inflammation. *Nat. Med.* **18**, 538–546.
- Hooper, L.V., Littman, D.R., and Macpherson, A.J. (2012). Interactions between the microbiota and the immune system. *Science* **336**, 1268–1273.
- Hotchkiss, R.S., and Karl, I.E. (2003). The pathophysiology and treatment of sepsis. *N. Engl. J. Med.* **348**, 138–150.
- Hubbard, W.J., Choudhry, M., Schwacha, M.G., Kerby, J.D., Rue, L.W., 3rd, Bland, K.I., and Chaudry, I.H. (2005). Cecal ligation and puncture. *Shock* **24** (1), 52–57.
- Ivanov, I.I., Atarashi, K., Manel, N., Brodie, E.L., Shima, T., Karaoz, U., Wei, D., Goldfarb, K.C., Santee, C.A., Lynch, S.V., et al. (2009). Induction of intestinal Th17 cells by segmented filamentous bacteria. *Cell* **139**, 485–498.
- Iyer, S.S., Latner, D.R., Zilliox, M.J., McCausland, M., Akondy, R.S., Penaloza-Macmaster, P., Hale, J.S., Ye, L., Mohammed, A.U., Yamaguchi, T., et al. (2013). Identification of novel markers for mouse CD4(+) T follicular helper cells. *Eur. J. Immunol.* **43**, 3219–3232.
- Johansen, F.E., Pekna, M., Norderhaug, I.N., Haneberg, B., Hietala, M.A., Krajci, P., Betsholtz, C., and Brandtzaeg, P. (1999). Absence of epithelial immunoglobulin A transport, with increased mucosal leakiness, in polymeric immunoglobulin receptor/secretory component-deficient mice. *J. Exp. Med.* **190**, 915–922.
- Johnston, R.J., Poholek, A.C., DiToro, D., Yusuf, I., Eto, D., Barnett, B., Dent, A.L., Craft, J., and Crotty, S. (2009). Bcl6 and Blimp-1 are reciprocal and antagonistic regulators of T follicular helper cell differentiation. *Science* **325**, 1006–1010.
- Kawamoto, S., Tran, T.H., Maruya, M., Suzuki, K., Doi, Y., Tsutsui, Y., Kato, L.M., and Fagarasan, S. (2012). The inhibitory receptor PD-1 regulates IgA selection and bacterial composition in the gut. *Science* **336**, 485–489.
- Kirkland, D., Benson, A., Mirpuri, J., Pifer, R., Hou, B., DeFranco, A.L., and Yarovinsky, F. (2012). B cell-intrinsic MyD88 signaling prevents the lethal dissemination of commensal bacteria during colonic damage. *Immunity* **36**, 228–238.
- Lécuyer, E., Rakotobe, S., Lengliné-Garnier, H., Lebreton, C., Picard, M., Juste, C., Fritzen, R., Eberl, G., McCoy, K.D., Macpherson, A.J., et al. (2014). Segmented filamentous bacterium uses secondary and tertiary lymphoid tissues to induce gut IgA and specific T helper 17 cell responses. *Immunity* **40**, 608–620.
- Linterman, M.A., Pierson, W., Lee, S.K., Kallies, A., Kawamoto, S., Rayner, T.F., Srivastava, M., Divekar, D.P., Beaton, L., Hogan, J.J., et al. (2011). Foxp3+ follicular regulatory T cells control the germinal center response. *Nat. Med.* **17**, 975–982.

- Littman, D.R., and Pamer, E.G. (2011). Role of the commensal microbiota in normal and pathogenic host immune responses. *Cell Host Microbe* 10, 311–323.
- Lozupone, C.A., Stombaugh, J.I., Gordon, J.I., Jansson, J.K., and Knight, R. (2012). Diversity, stability and resilience of the human gut microbiota. *Nature* 489, 220–230.
- Macpherson, A.J., and Harris, N.L. (2004). Interactions between commensal intestinal bacteria and the immune system. *Nat. Rev. Immunol.* 4, 478–485.
- Macpherson, A.J., and Uhr, T. (2004). Induction of protective IgA by intestinal dendritic cells carrying commensal bacteria. *Science* 303, 1662–1665.
- McLay, J., Leonard, E., Petersen, S., Shapiro, D., Greenspan, N.S., and Schreiber, J.R. (2002). Gamma 3 gene-disrupted mice selectively deficient in the dominant IgG subclass made to bacterial polysaccharides. II. Increased susceptibility to fatal pneumococcal sepsis due to absence of anti-polysaccharide IgG3 is corrected by induction of anti-polysaccharide IgG1. *J. Immunol.* 168, 3437–3443.
- Morita, R., Schmitt, N., Bentebibel, S.E., Ranganathan, R., Bourdery, L., Zurawski, G., Foucat, E., Dullaers, M., Oh, S., Sabzghabaei, N., et al. (2011). Human blood CXCR5(+)CD4(+) T cells are counterparts of T follicular cells and contain specific subsets that differentially support antibody secretion. *Immunity* 34, 108–121.
- Muegge, B.D., Kuczynski, J., Knights, D., Clemente, J.C., González, A., Fontana, L., Henrissat, B., Knight, R., and Gordon, J.I. (2011). Diet drives convergence in gut microbiome functions across mammalian phylogeny and within humans. *Science* 332, 970–974.
- Muramatsu, M., Kinoshita, K., Fagarasan, S., Yamada, S., Shinkai, Y., and Honjo, T. (2000). Class switch recombination and hypermutation require activation-induced cytidine deaminase (AID), a potential RNA editing enzyme. *Cell* 102, 553–563.
- Noverr, M.C., and Huffnagle, G.B. (2004). Does the microbiota regulate immune responses outside the gut? *Trends Microbiol.* 12, 562–568.
- Nurieva, R.I., Chung, Y., Martinez, G.J., Yang, X.O., Tanaka, S., Matskevitch, T.D., Wang, Y.H., and Dong, C. (2009). Bcl6 mediates the development of T follicular helper cells. *Science* 325, 1001–1005.
- Oltvai, Z.N., Milliman, C.L., and Korsmeyer, S.J. (1993). Bcl-2 heterodimerizes in vivo with a conserved homolog, Bax, that accelerates programmed cell death. *Cell* 74, 609–619.
- Pamer, E.G. (2004). Immune responses to *Listeria monocytogenes*. *Nat. Rev. Immunol.* 4, 812–823.
- Peterson, D.A., McNulty, N.P., Guruge, J.L., and Gordon, J.I. (2007). IgA response to symbiotic bacteria as a mediator of gut homeostasis. *Cell Host Microbe* 2, 328–339.
- Rittirsch, D., Huber-Lang, M.S., Flierl, M.A., and Ward, P.A. (2009). Immunodesign of experimental sepsis by cecal ligation and puncture. *Nat. Protoc.* 4, 31–36.
- Sait, L.C., Galic, M., Price, J.D., Simpfendorfer, K.R., Diavatopoulos, D.A., Uren, T.K., Janssen, P.H., Wijburg, O.L., and Strugnell, R.A. (2007). Secretory antibodies reduce systemic antibody responses against the gastrointestinal commensal flora. *Int. Immunol.* 19, 257–265.
- Schena, F., Volpi, S., Faliti, C.E., Penco, F., Santi, S., Proietti, M., Schenk, U., Damonte, G., Salis, A., Bellotti, M., et al. (2013). Dependence of immunoglobulin class switch recombination in B cells on vesicular release of ATP and CD73 ectonucleotidase activity. *Cell Rep.* 3, 1824–1831.
- Schenk, U., Westendorf, A.M., Radaelli, E., Casati, A., Ferro, M., Fumagalli, M., Verderio, C., Buer, J., Scanziani, E., and Grassi, F. (2008). Purinergic control of T cell activation by ATP released through pannexin-1 hemichannels. *Sci. Signal.* 1, ra6.
- Schenk, U., Frascoli, M., Proietti, M., Geffers, R., Traggiai, E., Buer, J., Ricordi, C., Westendorf, A.M., and Grassi, F. (2011). ATP inhibits the generation and function of regulatory T cells through the activation of purinergic P2X receptors. *Sci. Signal.* 4, ra12.
- Shroff, K.E., Meslin, K., and Cebra, J.J. (1995). Commensal enteric bacteria engender a self-limiting humoral mucosal immune response while permanently colonizing the gut. *Infect. Immun.* 63, 3904–3913.
- Shulzhenko, N., Morgun, A., Hsiao, W., Battle, M., Yao, M., Gavrillova, O., Orandle, M., Mayer, L., Macpherson, A.J., McCoy, K.D., et al. (2011). Crosstalk between B lymphocytes, microbiota and the intestinal epithelium governs immunity versus metabolism in the gut. *Nat. Med.* 17, 1585–1593.
- Slack, E., Balmer, M.L., Fritz, J.H., and Hapfelmeier, S. (2012). Functional flexibility of intestinal IgA - broadening the fine line. *Front. Immunol.* 3, 100.
- Sun, C.M., Hall, J.A., Blank, R.B., Bouladoux, N., Oukka, M., Mora, J.R., and Belkaid, Y. (2007). Small intestine lamina propria dendritic cells promote de novo generation of Foxp3 T reg cells via retinoic acid. *J. Exp. Med.* 204, 1775–1785.
- Suzuki, K., Meek, B., Doi, Y., Muramatsu, M., Chiba, T., Honjo, T., and Fagarasan, S. (2004). Aberrant expansion of segmented filamentous bacteria in IgA-deficient gut. *Proc. Natl. Acad. Sci. USA* 101, 1981–1986.
- Taylor, S.R., Gonzalez-Begne, M., Dewhurst, S., Chimini, G., Higgins, C.F., Melvin, J.E., and Elliott, J.I. (2008). Sequential shrinkage and swelling underlie P2X7-stimulated lymphocyte phosphatidyserine exposure and death. *J. Immunol.* 180, 300–308.
- Tsuji, M., Komatsu, N., Kawamoto, S., Suzuki, K., Kanagawa, O., Honjo, T., Hori, S., and Fagarasan, S. (2009). Preferential generation of follicular B helper T cells from Foxp3+ T cells in gut Peyer's patches. *Science* 323, 1488–1492.
- Ubeda, C., Taur, Y., Jenq, R.R., Equinda, M.J., Son, T., Samstein, M., Viale, A., Succi, N.D., van den Brink, M.R., Kamboj, M., and Pamer, E.G. (2010). Vancomycin-resistant *Enterococcus* domination of intestinal microbiota is enabled by antibiotic treatment in mice and precedes bloodstream invasion in humans. *J. Clin. Invest.* 120, 4332–4341.
- Vaishnava, S., Yamamoto, M., Severson, K.M., Ruhn, K.A., Yu, X., Koren, O., Ley, R., Wakeland, E.K., and Hooper, L.V. (2011). The antibacterial lectin RegIIIgamma promotes the spatial segregation of microbiota and host in the intestine. *Science* 334, 255–258.
- Wei, M., Shinkura, R., Doi, Y., Maruya, M., Fagarasan, S., and Honjo, T. (2011). Mice carrying a knock-in mutation of *Aicda* resulting in a defect in somatic hypermutation have impaired gut homeostasis and compromised mucosal defense. *Nat. Immunol.* 12, 264–270.
- Wilhelm, K., Ganesan, J., Müller, T., Dürr, C., Grimm, M., Beilhack, A., Krempf, C.D., Sorichter, S., Gerlach, U.V., Jüttner, E., et al. (2010). Graft-versus-host disease is enhanced by extracellular ATP activating P2X7R. *Nat. Med.* 16, 1434–1438.
- Wollenberg, I., Agua-Doce, A., Hernández, A., Almeida, C., Oliveira, V.G., Faro, J., and Graca, L. (2011). Regulation of the germinal center reaction by Foxp3+ follicular regulatory T cells. *J. Immunol.* 187, 4553–4560.
- Yu, D., Rao, S., Tsai, L.M., Lee, S.K., He, Y., Sutcliffe, E.L., Srivastava, M., Linterman, M., Zheng, L., Simpson, N., et al. (2009). The transcriptional repressor Bcl-6 directs T follicular helper cell lineage commitment. *Immunity* 31, 457–468.
- Zabel, B.A., Agace, W.W., Campbell, J.J., Heath, H.M., Parent, D., Roberts, A.I., Ebert, E.C., Kassam, N., Qin, S., Zovko, M., et al. (1999). Human G protein-coupled receptor GPR-9-6/CC chemokine receptor 9 is selectively expressed on intestinal homing T lymphocytes, mucosal lymphocytes, and thymocytes and is required for thymus-expressed chemokine-mediated chemotaxis. *J. Exp. Med.* 190, 1241–1256.